Full Paper

Wiley Online Library

ELECTROANALYSIS

DOI: 10.1002/elan.201800539

An Improved Design and Versatile New Lamination Fabrication Method for Twin Electrode Thin Layer Cells Utilizing Track-Etch Membranes

Adam Hauke,[a] Said Ehrlich,[b] Leanna Levine,[b] and Jason Heikenfeld*[a]

Abstract: Reported here are laminated membrane electrodes, an improved design and more advantageous method of fabrication for previously reported thin layer cell electrode systems developed on track-etch membranes. The laminated membrane approach potentially further improves flow resistance by dramatically reducing the surface area to volume ratio, but also produces a cohesive device that can be more readily applied to a broad range of applications. In addition, this new fabrication method was implemented in a scalable, commercial process and resulting product demonstrations indicate that volume manufacturing is feasible. Characterization of laminated membrane electrodes reveal redox cycling amplification factors as high as 30 with linear responses to variable concentrations of redox couple. These performance characteristics are shown to be comparable to similar generator-collector systems fabricated through much more laborious laboratory methods. This combination of added versatility, cost-reduced fabrication and exceptional performance clearly reveals unrealized potential of track-etch membrane approaches and boosts their candidacy as powerful new options for generator-collector electrode systems.

Keywords: thin layer cell · redox cycling · generator-collector electrodes · membrane · microfabrication

1 Introduction

Miniaturized sensing applications frequently rely on electrochemical detection methods due to the relative simplicity of their miniaturization and integration with microfluidic components [1–3]. The limiting factor to how small an electrochemical sensor can be made is often determined by the magnitude of its signal response which diminishes with the loss of surface area inherent in miniaturization. Generator-collector electrodes (GCEs) leverage an electrochemical mechanism known as redox cycling to mitigate this signal attenuation problem [4–6]. In GCEs, redox cycling occurs by polarizing the generator electrode such that a nearby reversible redox active species changes its oxidation state (oxidizes or reduces) before quickly transporting to the collector electrode which is polarized to cause the complementary change of state (Figure 1a). This is highly favorable compared to traditional single working electrode systems where only a single electron exchange occurs for single redox-active particle [6]. The resultant increased rate of electron exchange by rapid transport between these electrodes (i.e. cycling) amplifies the steady state current [7].

The magnitude of GCEs current enhancement is dictated by the efficiency of mass transport between these electrodes. Thus, a diverse assortment of GCEs have been developed, each aiming to optimize mass transport by utilizing various strategies (e.g. forced convection and favorable electrode geometry) [7]. It follows that GCEs which rely solely on diffusive analyte transport require the electrodes to be fabricated within microscale proximity to each other (i.e. with miniscule analyte diffusion lengths) [8]. One such solution is the twin electrode thin layer cell (TETLC) [9]. TETLCs consist of planar electrodes oriented such that they are geometrically parallel and facing each other, thereby confining a "thin layer" of sample between the electrodes (Figure 1a). Minimizing the spacing between these electrodes has been an ongoing research effort. While TETLCs have been used for decades to study kinetics of quiescent solutions [10–15], more recently, they have been deployed as amperometric detectors in microfluidic flow-through cell applications [16–18]. As the applied micro- and nano-fluidics fields continue to drive device requirements toward more extreme feature sizes (i.e. nanoscale TETLC electrode separation) [19,20], designers will need to address the increased fluid flow resistance inherent in decreasing closed channel dimensions as well as additional complex-

[a] A. Hauke, J. Heikenfeld
Novel Devices Laboratory
School of Electronics and Computing Systems
University of Cincinnati
Cincinnati, Ohio 45221, USA
E-mail: heikenjc@ucmail.uc.edu
[b] S. Ehrlich, L. Levine
ALine, Inc., Accelerated Microfluidic Development
Rancho Dominguez, California 90220, USA

Supporting information for this article is available on the WWW under https://doi.org/10.1002/elan.201800539

© 2018 Wiley-VCH Verlag GmbH & Co. KGaA, Weinheim

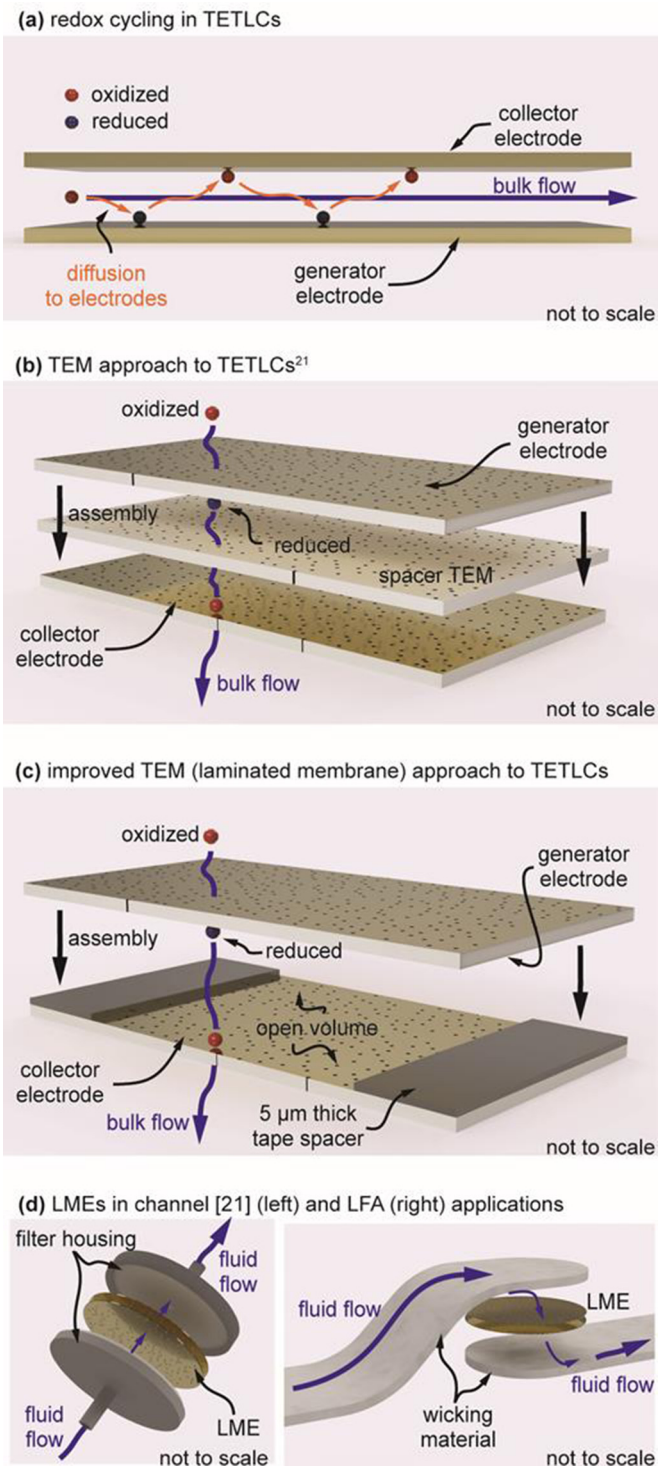


Fig. 1. Twin electrode thin layer cell (TETLC) configurations (a) a conventional TETLC depicting analyte transport in-plane with the electrodes; (b) the track-etch membrane (TEM) approach to TETLCs [21]; (c) the improved TEM approach or laminated membrane electrodes or LMEs (note that the amplification data presented in this article was collected with fluid sample in stopped-flow conditions and not as depicted here); (d) depictions of LMEs in integrated channel (left) [21] and lateral flow assay (LFA) applications (right).

ity and expense of integration with other system components.

A unique flow-through TETLC with an alternative flow geometry was introduced by Mizuguchi et al in 2012 [21]. Here, microporous electrodes were created on track-etch membrane filters (TEMs) (Figure 1b) and assembled using a third, non-conductive TEM as a spacer. In this device, fluid flow is directed orthogonally through the electrode surfaces facilitated by their open pores, as opposed to in-plane between the electrodes as in the conventional closed-channel designs (Figure 1a). This clever combination of low-cost materials and simple fabrication not only provides improved flow resistance, but also simplicity of integration into miniature analytical systems such as lab-on-chip. Importantly, these devices ensure analytes are transported within several µm of the electrode surfaces which could potentially produce faster sensor response times when applied to advective flow applications, overcoming diffusion limited transport limitations associated with conventional microchannel integration. Mizuguchi et al. further demonstrated the biosensing ability of this technology by applying it as an enzyme reactor in a combination glucose and lactate sensing device [22]. More recently, a similar device was reported that laminated porous platinum leaf electrodes with a TEM spacer using a lamination pouch [23].

Presented here, is an enhanced design for this new class of GCEs that provides for better flow conditions as well as a simple fabrication method that could be applied in volume manufacturing of versatile preassembled devices. These laminated membrane electrodes (LMEs) are assembled by laminating two gold coated TEMs using an ultra-thin (5 µm) double-sided tape as the spacer (Figure 1c). Laser cut patterns in the tape span large open areas between the electrodes as compared to the TEM spacer method. Eliminating the spacer TEM reduces unnecessary flow resistance caused by constricting the fluid path through its micropores and increases access for analyte in the bulk sample to cycle between the electrodes. Additionally, by using an adhesive spacer, adhesion of the electrodes is also achieved which results in a cohesive device that can be more readily deployed to a broader range of applications than the previously demonstrated flow channel (e.g. lateral flow assays, Figure 1d). Furthermore, the lamination method and added adhesion combine to facilitate volume manufacturing (e.g. roll-to-roll processes) of more versatile TETLCs. This manufacturability is demonstrated in a batch process by an industrial microfluidics manufacturing company ALine, Inc. We show these devices to produce 30-fold redox cycling amplification and calibration curves reveal remarkably linear responses to change in concentration, rivalling and surpassing the performance of other GCEs. This improved design and manufacturability greatly enhances the potential impact of this compelling new option for electrochemical sensor technology.

© 2018 Wiley-VCH Verlag GmbH & Co. KGaA, Weinheim

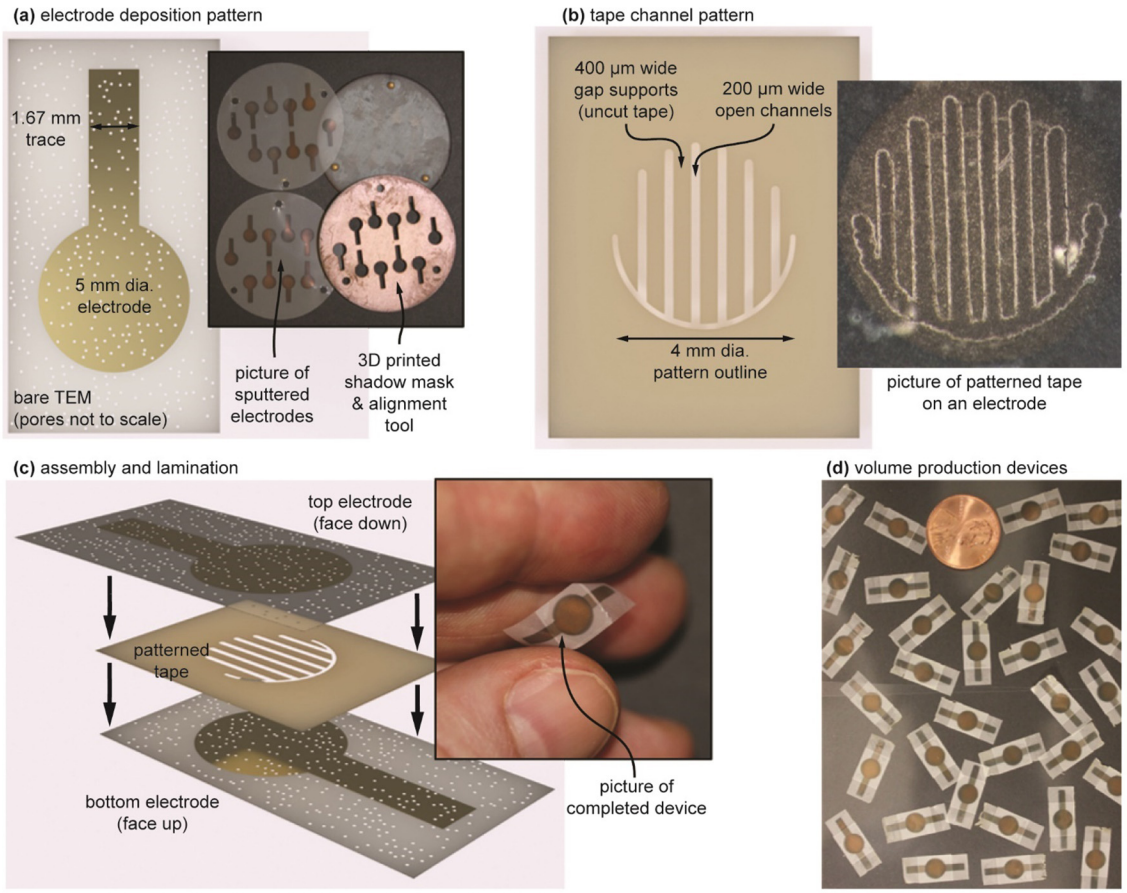


Fig. 2. Process for fabricating a laminated membrane electrode (LME) and inset pictures (a) gold electrodes patterned on a track etch membrane (TEM) (note that track etch membrane pores are not to scale in the illustration); (b) laser cut patterns for double sided tape with inset picture of patterned tape on an electrode; (c) final assembly for lamination with inset picture of a completed LME; (d) batch fabricated devices courtesy of ALine, Inc.

2 Experimental

2.1 LME Fabrication

All LMEs were produced with polyester track-etch membranes (47 mm discs, 3 µm diameter pores, 2×106 pores/cm^2, 9 µm thick, obtained from AR Brown-US). These membranes were sputter-coated (Denton Desk II) with 20 nm thick gold electrodes patterned using a 3D printed (Formlab 2) shadow mask (Figure 2a). Handmade laboratory devices were constructed (such that academic labs can repeat this work), and devices were also constructed by a commercial vendor (A-Line Inc., such that users can simply purchase devices for use).

The handmade LMEs fabricated in the lab at the University of Cincinnati (hereafter referred to as Lab LMEs) were fabricated individually by first cutting the gold coated track-etch membranes (Figure 2a) into 10 individual electrodes using a razor blade and straight edge. An array of fluid channels (Figure 2b) was laser cut (Universal Laser VLS3.50) in 5 µm thick electronic double-sided tape (3M 82600) with both protective liners still attached (this reduces ablation damage to the cut edges of the tape). After removing one protective liner (removed in the direction from top to bottom of the pattern as viewed in Figure 2b), the patterned tape was laminated onto an electrode before peeling off the second protective liner. A second electrode was then applied to the other side of the tape and the entire assembly was laminated (Western Magnum XRL-120) at 60 psi (note that although the laminator was used, simply pinching the assembly between the fingers has also been validated as a capable benchtop method). Figure 2c depicts the LME assembly stack with inset picture of the flexible final. product. This process can be summarized into three simple steps: (1) sputter; (2) laser cut; (3) laminate.

Maintaining the structure of such a thin material and small features when transferring to the electrodes drove the design of the pattern. Small standalone features (e.g. an array of small independent columns of tape) were initially attempted but would remain adhered to the first protective liner when removed (presumably due to fusion of the tape to the liner by laser ablation). This led to the design of the contiguous rows of tape which solved the issue, provided that the liner was removed from the side in which the rows were connected and proceeded toward the open end. If removed in other directions, open ends of

© 2018 Wiley-VCH Verlag GmbH & Co. KGaA, Weinheim

the rows tended to remain adhered to the protective liner (as with the standalone features) and would ultimately detach in an uncontrollable manner. Additionally, if patterned too thin, the rows would break off and remain adhered to the liner regardless of the direction of removal. This defined the 400 μm optimized width. The optimal 200 μm gap widths between the rows of tape provided the maximum unobstructed interelectrode volume while still providing the necessary separation of the generator and collector electrodes. Widths as large as 250 μm were successful but resulted in lower yield (see Discussion section for more details).

LMEs produced by co-authors at ALine, Inc. in the preliminary manufacturing feasibility study (hereafter referred to as Industry LMEs) are shown Figure 2d. For these prototypes, the track-etch membranes patterned with 10 electrodes each (Figure 2a) were processed at one time (10 LMEs made in one lamination process). The reader should note that these devices were fabricated with a different channel pattern (illustration provided in the supplementary data Figure S1) than that depicted in Figure 2a. An array of close packed circular channels was chosen to simplify the manufacturing process.

2.2 Testing

Potassium ferricyanide (Acros Organics 99 + %) was used to provide the ferri/ferrocyanide redox couple and solutions were all prepared in 0.5 mM phosphate buffer saline (Fisher PBS 1X, pH 7.4). The electrochemical cell used the LME electrodes as generator and collector electrodes with a solid-state Ag/AgCl reference electrode and a Pt wire counter electrode (eDAQ ET072 and BASi MW1038, respectively). A custom test platform was 3D printed (Formlab 2) to provide control and repeatability for setting up the cell and is shown in Figure 3. Testing was performed using stopped-flow conditions in order to determine the maximum redox cycling amplification. Test solution was applied to the top of the LMEs in a 15 μL droplet. The reference and counter electrodes were applied to the cell by inserting them into the meniscus of the droplet via the custom test platform (see zoom view in Figure 3). Cyclic voltammetry (CV) was performed by a bipotentiostat (two Gamry 600's connected and controlled via commercially available Gamry Biopotentiostat Control Cable and Gamry Framework software Biopotnetiostat Scripts) sweeping the generator (top LME electrode) from −0.05 to 0.5 V while holding the collector (bottom LME electrode) static at −0.05 V for a single cycle.

Amplification CV data was collected using 30 mM ferricyanide solution at several scan rates. Redox cycling signals were obtained in dual mode (DM) with the generator and collector electrodes connected appropriately to the bipotentiostat. Single mode (SM) data was collected by running the same test but with the collector electrode open circuited (bipotentiostat lead was disconnected from the bottom LME electrode) as is common in the literature [5,19,21,24,25].

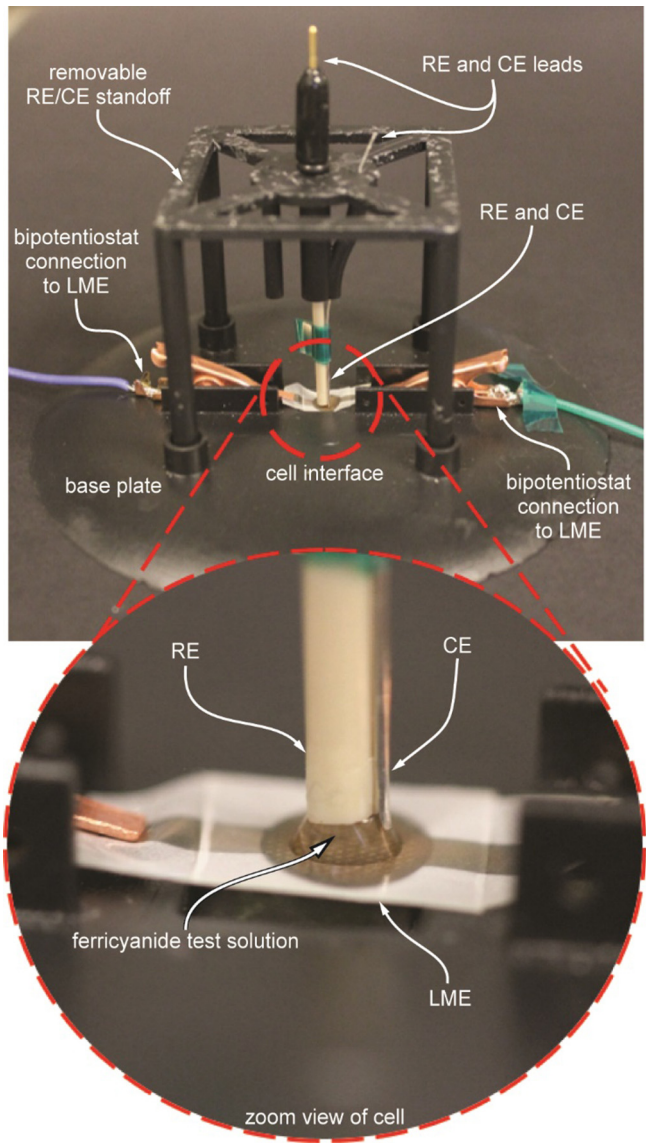


Fig. 3. The 3D printed test setup allowed removal and replacement of the reference and counter electrodes (RE and CE respectively) in a controlled and repeatable fashion.

Concentration response CV experiments were all performed at a 25 mV/s scan rate. The lowest concentration sample of test solution was tested first. Upon completion of the test, the reference and counter portion of the custom test platform (refer to Figure 3) was removed and the LME was lightly dabbed dry with a nonwoven tech wipe. A 15 μL droplet of the next larger concentration sample was applied, and the reference and counter portion of the custom test platform was replaced into the cell as described above. The next test was run, and this process repeated until all sample concentrations had been tested.

© 2018 Wiley-VCH Verlag GmbH & Co. KGaA, Weinheim

3 Results

Maintaining the structure of such a thin material and small features when transferring to the electrodes drove the design of the pattern. Small standalone features (e.g. an array of small independent columns of tape) were initially attempted but would remain adhered to the first protective liner when removed (presumably due to fusion of the tape to the liner by laser ablation). This led to the design of the contiguous rows of tape which solved the issue, provided that the liner was removed from the side in which the rows were connected together and proceeded toward the open end (top to bottom as viewed in Figure 2b and instructed in the Experimental section). If removed in other directions, open ends of the rows tended to remain adhered to the protective liner (as with the standalone features) and would ultimately detach in an uncontrollable manner. Additionally, if patterned too thin, the rows would break off and remain adhered to the liner regardless of the direction of removal. This defined the 400 μm optimized width. The optimal 200 μm gap widths between the rows of tape provided the maximum unobstructed interelectrode volume while still providing the necessary separation of the generator and collector electrodes. Widths as large as 250 μm were successfully demonstrated but resulted in low yield as discussed below.

All amplification factors (A) were calculated as $A = I_{G\text{-}DM}/I_{G\text{-}SM}$, the ratio of maximum generator current from DM ($I_{G\text{-}DM}$) to that from SM ($I_{G\text{-}SM}$). In all cases I_{DM} was achieved at 0.5 V (the upper scan limit) and I_{SM} near the characteristic limiting current voltage (~0.3 V), respectively. For the Lab LMEs, the slowest used scan rate of 5 mV/s produced the largest amplification factor of 29.6 (DM 0.876 mA to SM 0.0296 mA, Figure 4). Although amplification decreased quickly with scan rate, they remained significant with $A > 5.7$ for scan rates as high as 65 mV/s. (data provided in the supplementary data Table S.1). It is speculated that by using slower scan rates, each voltage scan cycle spends longer time intervals over which the generator is polarized near the limiting current voltage. This allows more time for analyte transfer between electrodes during redox cycling conditions and thereby facilitates an increased number of oxidation state changes for analytes during a given voltage scan cycle. So, although single mode limiting currents are lower (as is expected at slower scan rates), the relative level of dual mode redox cycling is enhanced and thus larger amplification factors are achieved. Lab LME amplification results were repeatable, although there was considerable device to device variation, producing amplification factors ranging from 15–30. Results reported here are for the single best performing device only.

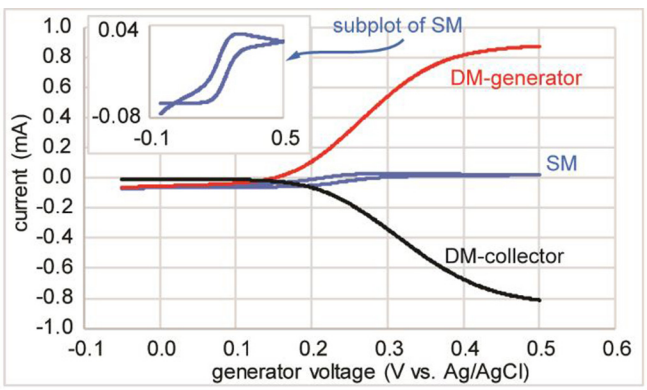


Fig. 4. Cyclic voltammagrams scanning the generator electrode from −0.05 to 0.5 V at a 5 mV/s scan rate in 30 mM ferricyanide solution result in a 30-fold amplification in peak signal from single mode (SM, collector open circuited from cell) to dual mode (DM, collector held static at −0.05 V) operation (inset subplot depicts SM curve). Only signal rise is shown for the DM curves for clarity.

LME concentration response was investigated over the range of 0.30 to 30 mM of ferricyanide and the raw data for the Lab LMEs is depicted in Figure 5a (all testing run at 25 mV/s scan rate). The curves are color coded by ferricyanide concentration with positive current swings corresponding to the generator and negative currents to the collector. Note that although the collector voltage was held static at −0.05 V, its response is shown as a function of the generator voltage. A collector efficiency value of 0.88 was determined by taking the average of efficiencies calculated at each concentration as the ratio of maximum adjusted collector current to maximum adjusted generator current (adjusted by shifting to zero the current at the start of the scans at −0.05 V). The response is more easily analyzed when viewing a plot of maximum collector current magnitude vs. concentration (Figure 5b) which reveals an R2 value of 0.98 and a 24 μA/mM sensitivity. The lowest tested concentration was 0.30 mM.

Data from Industry LMEs (made by co-authors at A-Line) is provided in the supplementary data Figure S.2. Amplification results were difficult to analyze due to distortion in the SM CV curves. The best result indicates an amplification factor of 22 (scan rate 25 mV/s in 3.0 mM ferricyanide). However, the DM tests produced similarly precise concentration responses to that of the hand fabricated LMEs with R2 values as high as of 0.997. A lower sensitivity of 5.1 μA/mM was likely due to fabrication concerns which are further discussed in the supplementary data file. A high rate of defects was apparent in the Industry LMEs as well as considerable device-to-device variation for those that did not fail. Short circuiting of the generator and collector was the most frequent failure mode. These issues for the Industry LMEs are likely resolvable with further work (see Discussion section), as the Industry LMEs were not as optimized in their fabrication process as the Lab LMEs.

4 Discussion

Characterization of the LMEs surpassed expectations with the 30-fold amplification and 0.88 collector efficiency that matches and often surpasses the performance of

© 2018 Wiley-VCH Verlag GmbH & Co. KGaA, Weinheim

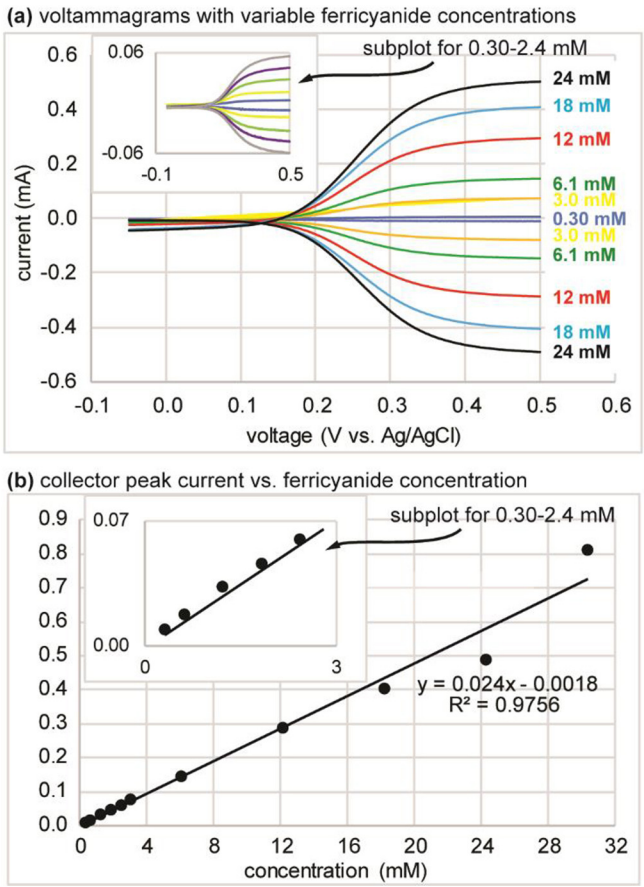


Fig. 5. Laminated membrane electrode responses for dual mode operation over 2 decades of ferricyanide concentrations (a) cyclic voltammagrams scanning the generator electrode from −0.05 to 0.5 V at a 5 mV/s scan rate while holding the collector electrode static at −0.05 V (only signal rise portion of curves shown for clarity) with generator signals swinging positive and collector signals swinging negative and shown as a function of the generator voltage (inset subplot depicts low concentrations); (b) plot of collector peak current (magnitude) vs. concentration from the voltammagrams is linear with R^2 value of 0.98 (inset subplot depicts low concentrations).

GCEs with similar sized electrode separation gaps and smaller (single μm gaps with 10- to 70-fold amplification at ≥0.90 collection. efficiency [26–28] and 50–250 nm gaps with 25- to 135-fold amplification [5,19,24,25]). It should be noted that all these comparable devices were fabricated by relatively laborious microfabrication techniques (e.g. electron beam lithography, photolithography, reactive ion etching, etc.). Aside from the considerable simplification in fabrication, LME devices and methods could also benefit end users by potential reduction in required sample volume and reduced resistance to fluid flow.

It is important to again emphasize, that the LME method is not a perfect substitute for photolithography. More variability is expected with the lamination process (e.g. laser cutting and tape thickness tolerances, etc.) and sub-micrometer feature sizes would be more difficult to achieve. Photolithographic techniques are preferential for more sophisticated devices where high precision and extremely small-scale feature sizes are required.

The large current responses of LMEs indicate that much smaller footprint LMEs could be employed for applications using similar redox couple concentrations. This could be a significant advantage of the increased open volume gaps and less restricted access to the electrode surfaces areas created by replacing the spacer TEM [21,22] by the patterned tape. A 4.76 mm^2 channel footprint provides a 24 nL sample gap volume for Lab LMEs while the Industry LME design results in a 40 nL volume (based on ideal fabrication dimensions; variability of tape thickness and laser cutting tolerances could produce variable volumes up to 50 nL). A 15 μL sample droplet was used simply for convenience in applying the reference and counter electrodes. Samples as small as 1 μL were shown to exhibit responses using no counter electrode and pressing the reference electrode directly against the top surface of the LME.

Future work should investigate integrating the reference and counter electrodes directly onto the devices. Integration of such electrodes is not a major challenge, as the reference and counter electrodes do not need to be in close proximity to the working electrodes. Such improvements would add more control of counter and reference electrode surface area which may have been a significant factor for the variation in performance. Further research should also characterize and optimize LME performance in flow through conditions as well as investigate the limits of detection. These considerations were not investigated here because they are not critical to primary advances demonstrated herein, and because such performance characteristics would be application dependent on methods of integration and sampling conditions.

Even further simplification in fabrication is now available as Sterlitech Corp., a leading producer of track-etch membranes, now offers membranes pre-coated with gold. Sourcing gold coated track-etch membranes would eliminate the sputtering process for an eventual LME manufacturer and further simplify processing. Electrode areas could simply be defined using the tape patterns without need for patterning the gold on the membranes. These design considerations will ultimately be application specific and should be the subject of future development.

Manufacturing yield and reliability should also be discussed. It should be noted that all results reported above for both the Lab LMEs and Industry LMEs were recorded on single devices from each respective lot. Although repeated results were obtained, defects and non-ideal behavior were also apparent in other tested devices. Lab LMEs were nearly all fabricated without failures (short circuiting of generator and collector) and maintained proper electrode separation throughout testing. However, one out of six of the Industry LMEs would electrically short after fabrication. Furthermore, two out of three of those remaining functional Industry LMEs shorted quickly after addition of sample solution. As the

© 2018 Wiley-VCH Verlag GmbH & Co. KGaA, Weinheim

track-etch membrane substrates are highly flexible, we speculate that sag of the membranes and electrodes occurs in the channels. Additionally, capillary forces can cause the substrates to pull together, bringing the electrodes even closer together when liquid sample is applied. Although this decrease in electrode separation could be leveraged to increase amplification, short-circuiting of the two electrodes also becomes increasingly probable. Therefore, the 250 μm gap width of the Industry LMEs is probably on the edge of reliability for LMEs reported here, and shorter gap widths would likely eliminate the observed electrical shorting.

Other non-ideal behavior such as distorted CV curves were produced by some LMEs fabricated by either method. Most variability issues are also likely caused by the fabrication processes. For instance, laser cutting tolerances are somewhat unpredictable. Deformation to the laser cut edges of the tape were confirmed to cause variable edge thicknesses from 5–10 μm. Additionally, incomplete laser cuts left notable tape residues over areas intended to be part of the electrochemically active surface area of the electrodes. More sophisticated means of tape patterning such as die cutting or higher precision lasers and further optimization of channel widths would likely reduce the variability and increase the yield of manufacturing devices. These fabrication process issues are to be expected at this early stage in development and the repeatable, exceptional performance of the successful LMEs gives confidence that these issues can be solved with further research.

Although LMEs already surpassed expectations, there is considerable room for improvements that could even further enhance their performance and versatility. The 3M 82600 electronics tape is not designed specifically for microfluidic applications and could contribute to adverse effects such as analyte exchange with the acrylic based adhesive and poor wettability in the gaps. It was chosen simply because it was the thinnest available solution. Development of custom ultra-thin microfluidic adhesive alternatives would be more ideal for lab-on-chip applications. Improvement efforts should focus on two considerations. First, decreasing the separation gap between the electrodes would enhance the redox cycling signal amplification factor, which is inversely proportional to the squared distance between the generator and collector [29]. Secondly, increasing the open channel width would increase the electrochemically active surface area of the electrodes per footprint area and thereby increase the overall signal response current density. This would effectively decrease the required footprint area of LMEs for a given application.

Other clever designs of LMEs are certainly possible and could be the subject of future experimentation. Two alternative design strategies were explored in this investigation which used separate methods for achieving the critical design requirements of adhesion and maintaining separation of the electrodes. The first strategy amends the existing TEM spacer method [21,22] by adhering the layered assembly by simply using a laser cutter to fuse the layers together (supplementary data Figure S.3a). Another more novel design used 5 μm diameter LCD spacer balls to maintain the gaps and an array of widely spaced adhesive columns patterned from an ultra-thin dry film photoresist or the electronics tape (supplementary Figure S.3b). Both alternatives demonstrated redox cycling behavior and exhibited their own advantages and disadvantages. As ease of manufacturing was the main focus of this research effort, the electronics tape method presented in this paper was ultimately chosen because of its superior simplicity in fabrication paired with relatively high-performance characteristics. However, further development of these and other alternative methods could yield even better results.

5 Conclusion

We have presented LMEs as an improved design concept and novel fabrication method for TETLCs utilizing TEM electrodes. This device not only matches the performance standards set by similarly sized GCEs but is also significantly simpler to fabricate. Amplification factors as large as 30 and a linear response to analyte concentration changes were demonstrated in these versatile devices. The lamination method introduced here eliminates need for complex microfabrication techniques and could translate well into industrial roll-to-roll fabrication methods. A leading industry expert in microfluidic device manufacturing produced batch fabricated prototype LMEs in a process that could potentially be adapted into a roll-to-roll volume fabrication process. This combination of expected performance, potential advantages in reduced sample volume and faster sensor response time, and simpler fabrication and integration offers GCE designers a desirable new alternative for sensing applications.

Conflict of Interest Statement

Corresponding author Jason Heikenfeld has an equity interest in Eccrine Systems, Inc., a company that may potentially benefit from the research results, and also serves on the company's Board. The terms of this arrangement have been reviewed and approved by the University of Cincinnati in accordance with its conflict of interest policies.

Acknowledgements

The authors would like to acknowledge support from the National Science Foundation and the industrial members of the Center for Advanced Design and Manufacturing of Integrated Microfluidics (NSF I/UCRC award number IIP-1738617). This research was supported in part by an appointment to the Student Research Participation Program at the U.S. Air Force Research Laboratory, 711th Human Performance Wing, Human Effectiveness Directorate, Human-Centered Intelligence, Surveillance and

 © 2018 Wiley-VCH Verlag GmbH & Co. KGaA, Weinheim

Reconnaissance Division administered by the Oak Ridge Institute for Science and Education through an interagency agreement between the U.S. Department of Energy and USAFRL. We would like to extend our thanks to Dr. William Heineman for lending his expertise in electrochemistry as well as to Dr. Gisela Lin, Dr. Abe Lee, and Dr. Ian Papautsky from the CADMIM organization for their additional support.

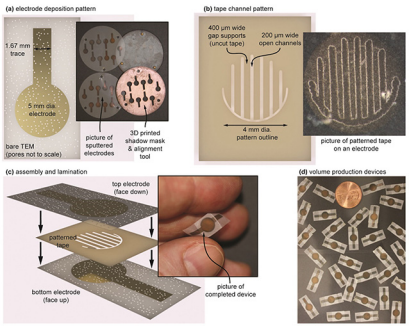
References

[1] S. Chen, L. Zhang, Y. Long, F. Zhou, *Electroanalysis* **2014**, *26*, 1236–1248.
[2] A. Tricoli, N. Nasiri, S. De, *Adv. Funct. Mater.* **2017**, *27*, 1605271.
[3] J. Heikenfeld, *Electroanalysis* **2016**, *28*, 1242–1249.
[4] C. G. Zoski, Ed., *Handbook of Electrochemistry*, Elsevier, **2007**.
[5] E. D. Goluch, B. Wolfrum, P. S. Singh, M. A. G. Zevenbergen, S. G. Lemay, *Anal. Bioanal. Chem.* **2009**, *394*, 447–456.
[6] T. Horiuchi, O. Niwa, M. Morita, H. Tabei, *J. Electrochem. Soc.* **1991**, *138*, 3549–3553.
[7] E. O. Barnes, G. E. M. Lewis, S. E. C. Dale, F. Marken, R. G. Compton, *Analyst* **2012**, *137*, 1068.
[8] J. H. Sluyters, *Recl. des Trav. Chim. des Pays-Bas* **1963**, *82*, 100–109.
[9] L. B. Anderson, C. N. Reilley, *J. Electroanal. Chem.* **1965**, *10*, 295–305.
[10] L. B. Anderson, C. N. Reilley, *J. Electroanal. Chem.* **1965**, *10*, 538–552.
[11] B. McDuffie, L. B. Anderson, C. N. Reilley, *Anal. Chem.* **1966**, *38*, 883–890.
[12] S. J. Konopka, B. McDuffie, *Anal. Chem.* **1970**, *42*, 1741–1746.
[13] B. J. Feldman, A. G. Ewing, R. W. Murray, *J. Electroanal. Chem. Interfacial Electrochem.* **1985**, *194*, 63–81.
[14] T. R. L. C. Paixão, E. M. Richter, J. G. A. Brito-Neto, M. Bertotti, *J. Electroanal. Chem.* **2006**, *596*, 101–108.
[15] T. R. L. C. Paixão, E. M. Richter, J. G. A. Brito-Neto, M. Bertotti, *Electrochem. Commun.* **2006**, *8*, 9–14.
[16] R. J. Fenn, S. Siggia, D. J. Curran, *Anal. Chem.* **1978**, *50*, 1067–1073.
[17] S. A. Brooks, R. T. Kennedy, *J. Electroanal. Chem.* **1997**, *436*, 27–34.
[18] G. E. M. Lewis, A. J. Gross, B. Kasprzyk-Hordern, A. T. Lubben, F. Marken, *Electrophoresis* **2015**, *36*, 1866–1871.
[19] M. A. G. Zevenbergen, B. L. Wolfrum, E. D. Goluch, P. S. Singh, S. G. Lemay, *J. Am. Chem. Soc.* **2009**, *131*, 11471–11477.
[20] S. Sarkar, K. Mathwig, S. Kang, A. F. Nieuwenhuis, S. G. Lemay, *Analyst* **2014**, *139*, 6052–6057.
[21] H. Mizuguchi, K. Shibuya, A. Fuse, T. Hamada, M. Iiyama, K. Tachibana, T. Nishina, J. Shida, *Talanta* **2012**, *96*, 168–173.
[22] H. Mizuguchi, K. Sasaki, H. Ichinose, S. Seino, J. Sakurai, M. Iiyama, T. Kijima, K. Tachibana, T. Nishina, T. Takayanagi, J. Shida, *Bull. Chem. Soc. Jpn.* **2017**, *90*, 1211–1216.
[23] H. R. Zafarani, L. Rassaei, E. J. R. Sudhölter, B. D. B. Aaronson, F. Marken, *Sensors Actuators B Chem.* **2018**, *255*, 2904–2909.
[24] C. Ma, L. P. Zaino III, P. W. Bohn, *Chem. Sci.* **2015**, *6*, 3173–3179.
[25] S. Partel, S. Kasemann, V. Matylitskaya, C. Thanner, C. Dincer, G. Urban, *Microelectron. Eng.* **2017**, *173*, 27–32.
[26] O. Niwa, M. Morita, H. Tabei, *Anal. Chem.* **1990**, *62*, 447–452.
[27] V. A. T. Dam, W. Olthuis, A. van den Berg, *Analyst* **2007**, *132*, 365.
[28] M. Morita, K. Hayashi, T. Horiuchi, S. Shibano, K. Yamamoto, K. J. Aoki, *J. Electrochem. Soc.* **2014**, *161*, H178–H182.
[29] M. G. Straver, M. Odijk, W. Olthuis, A. van den Berg, *Lab Chip* **2012**, *12*, 1548.

Received: August 1, 2018
Accepted: September 8, 2018
Published online on ■■, ■■■

 © 2018 Wiley-VCH Verlag GmbH & Co. KGaA, Weinheim

FULL PAPER



*A. Hauke, S. Ehrlich, L. Levine, J. Heikenfeld**

1 – 9

An Improved Design and Versatile New Lamination Fabrication Method for Twin Electrode Thin Layer Cells Utilizing Track-Etch Membranes